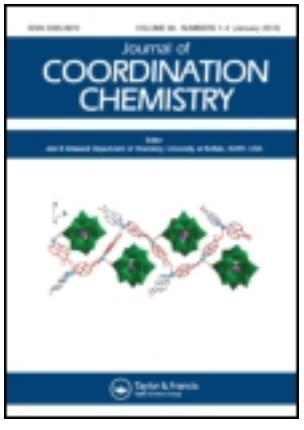


Journal of Coordination Chemistry
Publication details, including instructions for authors and subscription information:
http://www.tandfonline.com/loi/gcoo20

# Synthesis, characterization, and interaction with DNA of Cu(II) and Zn(II) complexes with 2,2′-bipyridyl-6,6′-dicarboxylic acid

Ya-Guang Sun [a], Ke-Long Li [a], Zhen-He Xu [a], Tian-Yi Lv [a], Shu-Ju Wang [a], Li-Xin You [a] & Fu Ding [a]
[a] Laboratory of Coordination Chemistry, Shenyang University of Chemical Technology, Shenyang, P.R. China
Published online: 21 Jun 2013.

To cite this article: Ya-Guang Sun, Ke-Long Li, Zhen-He Xu, Tian-Yi Lv, Shu-Ju Wang, Li-Xin You & Fu Ding (2013) Synthesis, characterization, and interaction with DNA of Cu(II) and Zn(II) complexes with 2,2′-bipyridyl-6,6′-dicarboxylic acid, Journal of Coordination Chemistry, 66:14, 2455-2464, DOI: 10.1080/00958972.2013.806655

To link to this article: http://dx.doi.org/10.1080/00958972.2013.806655

*Journal of Coordination Chemistry*, 2013
Vol. 66, No. 14, 2455–2464, http://dx.doi.org/10.1080/00958972.2013.806655



# Synthesis, characterization, and interaction with DNA of Cu(II) and Zn(II) complexes with 2,2′-bipyridyl-6, 6′-dicarboxylic acid

YA-GUANG SUN*, KE-LONG LI, ZHEN-HE XU, TIAN-YI LV, SHU-JU WANG, LI-XIN YOU and FU DING

Laboratory of Coordination Chemistry, Shenyang University of Chemical Technology, Shenyang, P.R. China

(*Received 14 November 2012; in final form 21 March 2013*)

Two transition metal complexes, $[Cu_2(bpdc)_2H_2O]\cdot 2H_2O$ (**1**) and $Zn(bpdc)(H_2O)_2$ (**2**) ($H_2bpdc = 2,2'$-bipyridine-6,6′-dicarboxylic acid), were synthesized and characterized by elemental analysis, IR spectroscopy, and single-crystal X-ray diffraction. Complex **1** is dinuclear with two five-coordinate cupric ions and **2** is mononuclear with one six-coordinate zinc. Interactions of **1** and **2** with DNA have been investigated using UV–Vis absorption spectra. The cleavage reaction on DNA has been monitored by agarose gel electrophoresis.

*Keywords*: Dinuclear complex; Mononuclear complex; DNA binding; DNA cleavage



## 1. Introduction

Interaction of transition metal complexes with DNA has been extensively studied because of diverse applications in molecular biology, biotechnology, and therapeutic agents [1–6]. Transition metal complexes with diverse structural features, redox behavior, and physicochemical properties are sensitive diagnostic agents as exemplified by bleomycins or cisplatin/carbo-platin in chemotherapeutic applications. Copper(II) and zinc(II) ions are redox active and play a crucial role in catalytic sites of oxidoreductases. Numerous copper and zinc complexes have been screened for their biological activities [7–10]. Mao and coworkers have synthesized zinc(II) complexes, which exhibit high nuclease activities towards cleavage of supercoiled plasmid DNA with the activity being maximum under physiological pH [11]. Hirota and coworkers found that $[Cu_2(m\text{-}CH_3COO)(m\text{-}H_2O)(m\text{-}OH)(phen)_2]^{2+}$ inhibits LDH activity and induces apoptosis selectively in human cancer cells with efficient hydrolytic cleavage activity [12]. Copper/zinc complexes have favorable anticancer activities. Furthermore, many complexes with the 2,2′-bipyridyl derivatives are potential antitumor agents [11, 13–16]. Recently, Gao and coworkers synthesized two dinuclear cobalt(II) complexes of 2,2′-dipyridyl derivatives, which exhibit cytotoxic activity against extracted HC-DNA and apoptotic effect on HeLa cells [17].

*Corresponding author. Email: yaguangsun@yahoo.com.cn

In this paper, we synthesized two transition metal complexes with 2,2′-dipyridyl dicarboxylate ligands. Herein, 2,2′-bipyridine-6,6′-dicarboxylic acid was used for constructing transition metal complexes $[Cu_2(bpdc)_2H_2O]\cdot 2H_2O$ (**1**) and $Zn(bpdc)(H_2O)_2$ (**2**). Complexes **1** and **2** have been characterized by FT-IR, elemental analysis, and single-crystal X-ray diffraction, and examined for interactions with CT-DNA via UV–Vis absorption spectra and agarose gel electrophoresis.

## 2. Experimental

### 2.1. *Materials*

All chemicals purchased were of reagent grade and used without purification. All syntheses were carried out in 25 mL Teflon-lined autoclaves under autogenous pressure. The reaction vessels were filled to 60% volume capacity. Water used in the reactions was distilled water.

### 2.2. *Synthesis of 1*

A mixture of $H_2$bpdc (0.2 mM, 0.0488 g), $Cu(NO_3)_2\cdot 3H_2O$ (0.2 mM, 0.0483 g), and $H_2O$ (10 mL) was placed in a 25-mL Teflon-lined autoclave and kept under autogenous pressure at 170 °C for 3 days, then cooled to room temperature at 10 °C $h^{-1}$. Blue square-shaped crystals of **1** were obtained with yield of 52%. Elemental analysis Calcd (%) for $C_{24}H_{20}Cu_2N_4O_{12}$: C, 42.19; H, 2.97; N, 8.20. Infrared absorption spectra were measured and the major absorption peaks were identified. IR spectrum (KBr, $cm^{-1}$) for **1**: 3464(s), 3094(w), 3068(w), 3050(w), 1665(s), 1644(s), 1604(s), 1579(m), 1477(w), 1411(s), 1396(s), 1360(s), 1277(m), 1214(m), 1184(w), 1079(w), 1008(w), 916(w), 839(m), 783(m), 694(m), 651(w), 577(w).

### 2.3. *Synthesis of 2*

A procedure identical with **1** was followed to prepare **2** except $Cu(NO_3)_2\cdot 3H_2O$ was replaced by $Zn(NO_3)_2\cdot 6H_2O$ (0.2 mM, 0.0595 g). The Teflon-lined autoclave was kept under autogenous pressure at 170 °C for three days, and then cooled at a rate of 10 °C $h^{-1}$. Colorless square-shaped crystals of **2** were obtained with a yield of 63%. Elemental analysis Calcd (%) for $C_{12}H_{10}ZnN_2O_6$: C, 41.96; H, 2.95; N, 8.16. IR spectrum (KBr, $cm^{-1}$) for **2**: 3248(s), 3088(s), 1624(s), 1595(s), 1576(s), 1426(s), 1385(s), 1277(m), 1197(w), 1166(w), 1088(w), 1028(w), 916(w), 849(w), 784(s), 718(w), 700(w), 683(w), 644(w), 579(w).

### 2.4. *Crystallographic analyses*

Crystallographic data of **1** and **2** were collected at 293 K on a Bruker SMART 1000 CCD diffractometer using monochromated MoKα radiation ($\lambda = 0.71073$ Å), applying the ω scan technique. An empirical absorption correction was applied. The structures were solved by direct methods and refined by full-matrix least-squares against $F^2$ using *SHELXS*-97 and *SHELXL*-97 [18, 19]. Anisotropic thermal parameters were assigned to all non-hydrogen atoms. Hydrogens were placed in calculated positions and refined as riding with fixed isotropic thermal parameters. Analytical expressions of neutral atom scattering factors were

Table 1. Crystallographic data and refinement summary for **1** and **2**.

| | | |
|---|---|---|
| Empirical formula | $C_{24}H_{20}Cu_2N_4O_{12}$ | $C_{12}H_{10}N_2O_6Zn$ |
| Formula weight | 683.54 | 343.59 |
| Color and habit | Green-blue | Colorless |
| Crystal system | Monoclinic | Monoclinic |
| Space group | $P2_1/c$ | $P2_1/c$ |
| $a$ [Å] | 8.3474 (12) | 8.246 (3) |
| $b$ [Å] | 21.010 (3) | 21.751 (8) |
| $c$ [Å] | 6.9696 (10) | 6.934 (3) |
| $\alpha$ [°] | 90 | 90 |
| $\beta$ [°] | 95.959 | 105.455 (4) |
| $\gamma$ [°] | 90 | 90 |
| $V$ (Å$^3$) | 1215.7 (3) | 1198.7 (8) |
| $Z$ | 2 | 4 |
| $T$ (K) | 293 (2) | 293 (2) |
| $\lambda$ (Å) | 0.71075 | 0.71073 |
| $D_{calcd}$ (g/cm$^3$) | 1.867 | 1.9040 (13) |
| $\mu$ (mm$^{-1}$) | 1.829 | 2.082 |
| GOF on $F_2$ | 1.139 | 1.049 |
| $R^a$, $wR^b$ [$I>2\sigma(I)$] | 0.0577, 0.1016 | 0.0334, 0.0669 |
| $R$, $wR$ (all data) | 0.0827, 0.1088 | 0.0426, 0.0705 |

[a] $R = \Sigma||F_o| - |F_c||/\Sigma|F_o|$.
[b] $wR = [\sum(F_0^2 - F_c^2)2/\sum w(F_0^2)^2]^{1/2}$.

Table 2. Selected bond distances (Å) and angles (°) for **1** and **2**.

| | | | |
|---|---|---|---|
| **1** | | | |
| Cu(1)–O(3)#1 | 1.896 (3) | Cu(1)–N(1) | 1.915 (3) |
| Cu(1)–O(2) | 2.020 (3) | Cu(1)–N(2) | 2.070 (3) |
| Cu(1)–O(5) | 2.207 (3) | | |
| O(3)#1–Cu(1)–N(1) | 168.61 (13) | O(3)#1–Cu(1)–O(2) | 95.56 (12) |
| N(1)–Cu(1)–O(2) | 80.62 (13) | O(3)#1–Cu(1)–N(2) | 102.66 (12) |
| N(1)–Cu(1)–N(2) | 79.93 (13) | O(2)–Cu(1)–N(2) | 160.00 (12) |
| O(3)#1–Cu(1)–O(5) | 93.25 (12) | N(1)–Cu(1)–O(5) | 97.56 (13) |
| O(2)–Cu(1)–O(5) | 91.53 (12) | N(2)–Cu(1)–O(5) | 95.55 (12) |
| **2** | | | |
| Zn(1)–O(3) | 2.4198 (17) | Zn(1)–O(6) | 2.3121 (16) |
| Zn(1)–O(4) | 1.9678 (18) | Zn(1)–N(1) | 2.1088 (18) |
| Zn(1)–O(5) | 2.0173 (16) | Zn(1)–N(2) | 2.1095 (19) |
| O(4)–Zn(1)–O(5) | 129.47 (7) | N(1)–Zn(1)–O(6) | 72.57 (7) |
| O(4)–Zn(1)–N(1) | 112.01 (7) | N(2)–Zn(1)–O(6) | 147.73 (6) |
| O(5)–Zn(1)–N(1) | 108.51 (7) | O(4)–Zn(1)–O(3) | 78.88 (6) |
| O(4)–Zn(1)–N(2) | 109.50 (7) | O(5)–Zn(1)–O(3) | 83.23 (6) |
| O(5)–Zn(1)–N(2) | 108.91 (7) | N(1)–Zn(1)–O(3) | 147.14 (6) |
| N(1)–Zn(1)–N(2) | 75.32 (7) | N(2)–Zn(1)–O(3) | 71.83 (6) |
| O(4)–Zn(1)–O(6) | 80.21 (6) | O(6)–Zn(1)–O(3) | 140.14 (5) |
| O(5)–Zn(1)–O(6) | 84.46 (6) | | |

employed and anomalous dispersion corrections were incorporated. The crystallographic data and selected bond lengths and angles for **1** and **2** are listed in tables 1 and 2, respectively.

## 3. Results and discussion

### 3.1. *Crystal structure of 1*

The atomic numbering scheme and atom connectivities for **1** are shown in figure 1. The structure was refined in the monoclinic crystal lattice with space group $P2_1/c$. The

molecular structure of **1** reveals two five-coordinate Cu(II) ions and the coordination geometry can be viewed as square-pyramidal, coordinated by two nitrogens (N1 and N2) from a bpdc and two oxygens (O2 and O3A) from two different bpdc ligands and one oxygen (O5) from coordinated water at the axial position. Cu–O distances are 1.896(3)–2.207(3) Å and the Cu–N distances are 1.915(3)–2.070(3) Å, in agreement with those observed for the five-/six-coordinate Cu in carboxylate complexes [20]. The coordinated water and free water are hydrogen donors, which form intermolecular hydrogen bonds [21–23] with uncoordinated oxygen of carboxylate in adjacent molecules (table 3). Intermolecular O–H···O hydrogen bonds extend the dinuclear structure into a 2-D network (figure 2). In addition, there are weak C–H···O hydrogen bonds involving O from coordinated carboxylate. The C···O separation is 3.284–3.372 Å with H···O distances of 2.358–2.478 Å. The weak C–H···O hydrogen bonds link the 2-D structure into a 3-D supramolecular structure. Both the coppers stay almost in the planes of the respective bipyridine rings. The distance between two Cu(II) ions is 5.265 Å.

### 3.2. *Crystal structure of 2*

The atom-numbering scheme and connectivities for **2** are shown in figure 3. The structure was refined in the monoclinic crystal lattice with space group $P2_1/c$. The molecular structure of **2** reveals one six-coordinate zinc with coordination geometry of a double cap square-pyramid, coordinated by two nitrogens (N1 and N2) from a bpdc and two oxygens (O3 and O6) from a bpdc, and two oxygens (O4 and O5) from two coordinated waters in axial positions. The Zn–O distances are 1.968(18)–2.420(17) Å and the Zn–N distances are 2.109(18) Å, in agreement with those observed [24]. The coordinated waters are hydrogen donors to form intermolecular hydrogen bonds [21–23] with uncoordinated oxygen of carboxylates in adjacent molecules (table 3). Intermolecular O–H···O hydrogen bonds extend the mononuclear structure into a 2-D network (figure 4). There are weak C–H···O hydrogen bonds involving coordinated carboxylate. The C···O separation is 3.191–3.224 Å with

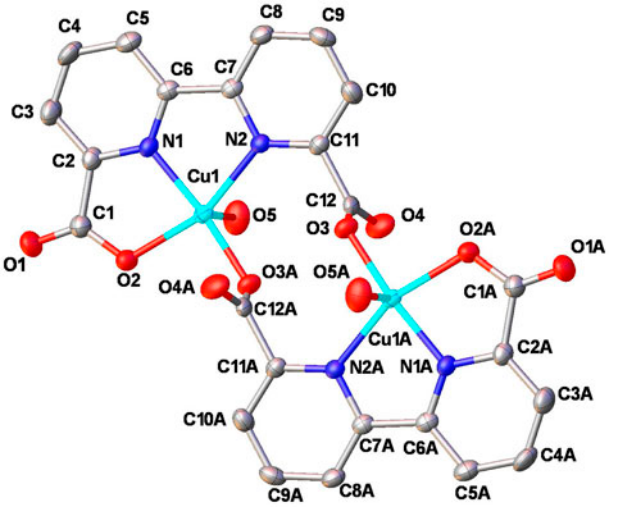


Figure 1. The coordination environments of Cu(II) in **1**.

Table 3. Hydrogen-bond geometry for **1** and **2**.

| Donor-H···acceptor | D–H | H···A | D···A | D–H···A | Symmetry code on A |
|---|---|---|---|---|---|
| **1** | | | | | |
| O(5)–H(5A)···O(4) | 0.84 | 2.00 | 2.8180 | 164 | $2-x, -y, -z$ |
| O(5)–H(5B)···O(1) | 0.84 | 2.06 | 2.8391 | 155 | $x, 1/2-y, -1/2+z$ |
| O(6)–H(6A)···O(2) | 0.85 | 2.04 | 2.8901 | 175 | $-1+x, y, z$ |
| O(6)–H(6B)···O(2) | 0.85 | 2.27 | 3.0897 | 163 | $-1+x, 1/2-y, 1/2+z$ |
| C(8)–H(8)···O(4) | 0.93 | 2.48 | 3.3712 | 161 | $-1+x, y, z$ |
| C(9)–H(9)···O(1) | 0.93 | 2.36 | 3.2849 | 174 | $1-x, -1/2+y, 1/2-z$ |
| C(10)–H(10)···O(6) | 0.93 | 2.44 | 3.3207 | 159 | $1-x, -y, 1-z$ |
| **2** | | | | | |
| O(4)–H(4A)···O(8) | 0.82 | 1.84 | 2.644 (2) | 167 | $x, 3/2-y, -1/2+z$ |
| O(4)–H(4B)···O(7) | 0.84 | 1.84 | 2.642 (2) | 161 | $1-x, 2-y, 1-z$ |
| O(5)–H(5A)···O(7) | 0.82 | 1.94 | 2.749 (2) | 171 | $1-x, 2-y, 2-z$ |
| O(5)–H(5B)···O(3) | 0.85 | 2.08 | 2.933 (2) | 179 | $x, 3/2-y, 1/2+z$ |
| C(5)–H(5)···O(6) | 0.93 | 2.31 | 3.223 (3) | 168 | $-1+x, y, z$ |
| C(9)–H(9)···O(8) | 0.93 | 2.28 | 3.192 (3) | 166 | $-x, 1/2+y, 3/2-z$ |

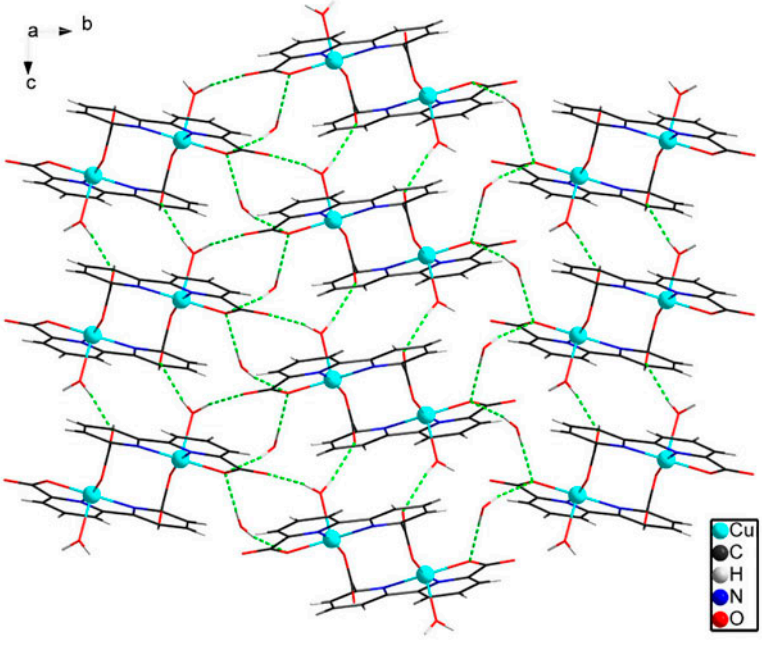


Figure 2. The 2-D structure formed by strong O–H···O hydrogen bonds in **1** (*green dashed lines* represent the H-bond (see http://dx.doi.org/10.1080/00958972.2013.806655 for color version).

H···O distances of 2.284–2.306 Å. The weak C–H···O hydrogen bonds link the 2-D structure into a 3-D supramolecular structure.

Compounds **1** and **2** were obtained by similar hydrothermal reactions with $Zn(NO_3)_2{\cdot}6H_2O$/$Cu(NO_3)_2{\cdot}3H_2O$, $H_2$bpdc, and $H_2O$, but **1** and **2** have different structures, ascribed to different coordination geometry of cupric and zinc ions, which drive the packing of the structure. For instance, six-coordinate Zn has two coordinated waters, resulting in bonds to the carboxylic acid oxygen atoms to be *trans* in **2**, compared to *cis* in **1**. Furthermore, having uncoordinated water in **1** contributes to the difference in packing.

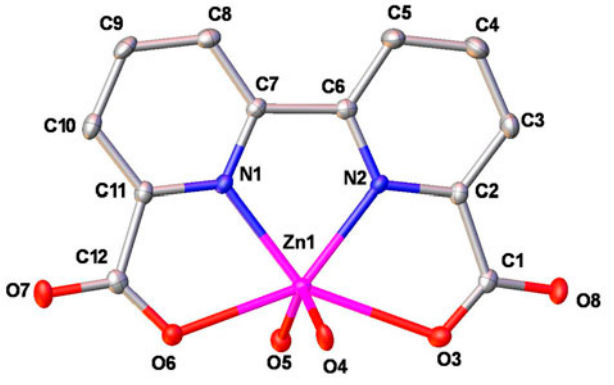


Figure 3. The coordination environments of Zn(II) in **2**.

### 3.3. *DNA binding*

The binding strength of the complexes with CT-DNA was examined by measuring its effects on the UV spectrum of DNA. As shown in figures 5 and 6, with concentration of CT-DNA increasing, a decrease in the absorption intensities of the $\pi$–$\pi^*$ absorption band of **1** and **2** with red shift in band positions is observed. The intrinsic binding constant ($K_b$) was determined with the following equation [25]:

$$[\mathrm{DNA}]/(\varepsilon_a - \varepsilon_f) = [\mathrm{DNA}]/(\varepsilon_b - \varepsilon_f) + 1/K_b(\varepsilon_b - \varepsilon_f)$$

where [DNA] is the concentration of CT-DNA in the base pairs, $\varepsilon_a$ is the apparent extinction coefficient obtained by calculating Aobs/[complex], $\varepsilon_f$ corresponds to the extinction coefficient of the complex in its free form, and $\varepsilon_b$ refers to the extinction coefficient of the

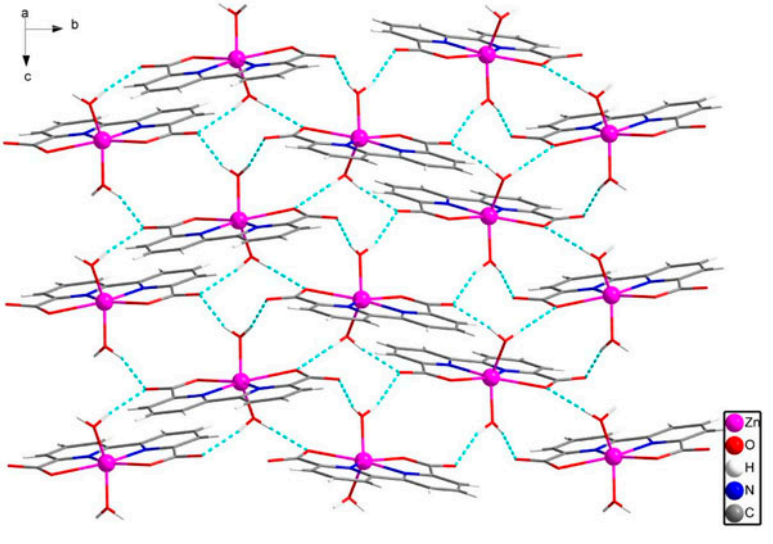


Figure 4. The 2-D structure formed by strong O–H···O hydrogen bonds in **2** (*blue dashed lines* represent the H-bond) (see http://dx.doi.org/10.1080/00958972.2013.806655 for color version).

complex in the bound form. Each set of data, when fitted to the above equation, gives a straight line with a slope of $1/(\varepsilon_b-\varepsilon_f)$ and intercept of $1/K_b(\varepsilon_b-\varepsilon_f)$; the ratio of the slope to intercept gives the value of the intrinsic binding constant. The intrinsic binding constants $K_b$ obtained for **1** and **2** were $2.17\times10^3$ and $6.58\times10^3$, respectively, lower than those observed [26–30] for the typical classical intercalator ethidium bromide (EthBr; $K_b$, $4.94\times10^5\,M^{-1}$ in a 25 mM Tris–HCl/40 mM NaCl buffer, pH 7.9). Therefore, the interaction of the two complexes with CT-DNA is considered to be weaker than with classical intercalators. These phenomena show that the complexes intercalate with DNA and the spectroscopic similarity suggests similar binding modes to DNA. However, the hypochromism for **2** is larger than that for **1**.

### 3.4. *DNA cleavage*

Pure pBR322 plasmid DNA/Hela DNA/KB DNA and the mixture of pBR322 plasmid DNA/Hela DNA/KB DNA with the complexes was loaded onto 1.5% agarose gel (stained by EtBr) and electrophoresis was carried out in 0.5 × TAE systems at 120 V for 2 h. The cleavage products were irradiated at room temperature with a UV lamp (365 nm, 10 W) and analyzed with a UVP GDS 8000 complete gel documentation and analysis system, equipped with Gel works 1 D version 3.00 software. From figure 7 and Supplementary material, we can see the agarose gel electrophoreses of **1** and **2**. We use the ability of complexes to perform Hela DNA/KB DNA/pBR322 plasmid DNA cleavage to study its degree or mode with DNA. Electrophoresis could make round Hela DNA/KB DNA/pBR322 plasmid DNA controlled. When it occurs, migration will be observed for the supercoiled form (Form I). With time, the supercoiled form (Form I) transforms to the nicked form (Form III and Form II) [15, 31–33]. In figure 7, Lane 0 is Marker; Lane 1 is DNA alone; Lanes 2–5 are (DNA + **1** with different concentrations); and Lanes 6–9 are (DNA + **2** with different concentration). With increasing concentration of Cu(II) or Zn(II) complexes, the intensity of the supercoiled DNA (Form I) relax to produce Form II and Form III. In general, the two complexes have biological activity cutting Hela DNA/KB DNA/pBR322 plasmid DNA into fragments. Their cleavage effect is weaker than that of Cu, Zn complexes in the

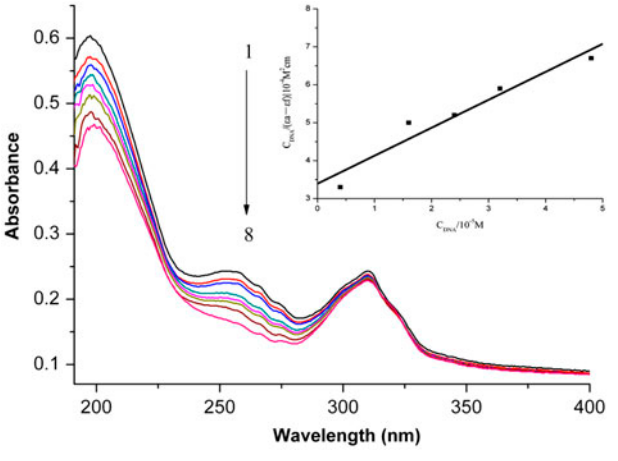


Figure 5. Absorption spectral traces of **1** in 5 mM Tris–HCl–NaCl buffer (pH = 7.4) in the absence (line 1) and the presence (lines 2–8) of increasing amounts of CT-DNA $C_{DNA}$ (lines 2–8): 4, 8, 16, 20, 24, 32 and 48 μM.

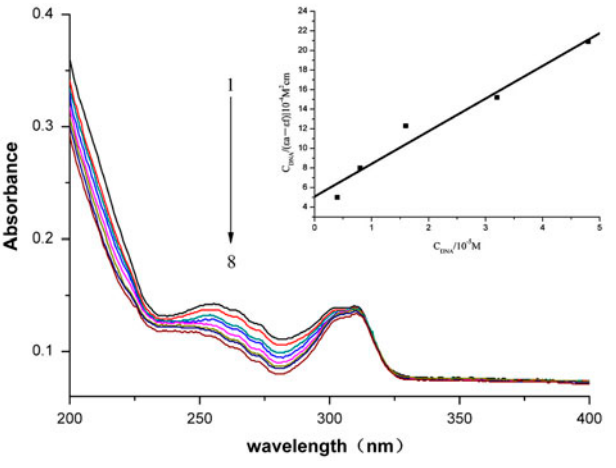


Figure 6. Absorption spectral traces of **2** in 5 mM Tris–HCl–NaCl buffer (pH = 7.4) in the absence (line 1) and presence (lines 2–8) of increasing amounts of CTDNA $C_{DNA}$ (lines 2–8): 4, 8, 16, 20, 24, 32 and 48 μM.

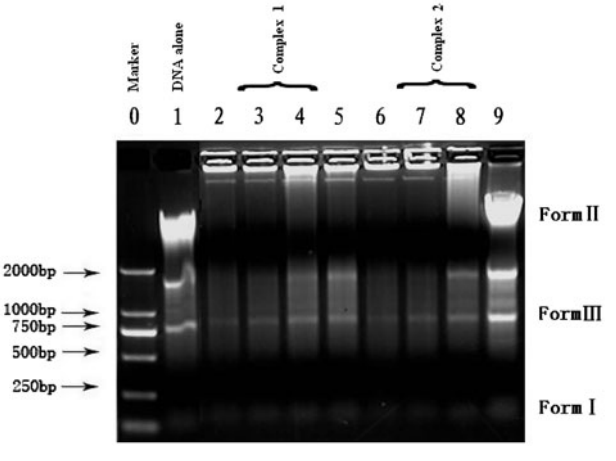


Figure 7. Cleavage of Hela DNA (10 μM) in the presence of complexes, Lane 0, Marker; Lane 1, DNA alone; Lanes 2–5, DNA + **1** (7.0, 14.0, 21.0 and 28.0 μM, respectively); Lanes 6–9, DNA + **2** (7.0, 14.0, 21.0 and 28.0 μM, respectively).

literature [34–36]. This may be because $H_2$bpdc conjugate plane is smaller. DNA cleavage of **1** and **2** is similar. To ascertain which section of **1** is playing a major role in DNA cleavage, the DNA cleavage of metal, ligand, and **1** is investigated (Supplementary material). The present results show that ligand is much more important than metal in DNA cleavage.

## 4. Conclusion

Dinuclear $[Cu_2(bpdc)_2H_2O]\cdot 2H_2O$ (**1**) and mononuclear $Zn(bpdc)(H_2O)_2$ (**2**) derived from bipyridine-dicarboxylic acid ligands have been synthesized and characterized. Structures of **1** and **2** were determined by X-ray crystallography. DNA interaction by absorption spectral

studies showed interaction. This molecule exhibited nuclease activity in the absence of any oxidizing or reducing agents. The cleavage efficiency was dependent on the complex concentration.

## Supplementary data

CCDC 901007 (**1**) and 901006 (**2**) contain the supplementary crystallographic data of this paper. These data can be obtained via the Cambridge Crystallographic Data Center (E-mail: deposit@ccdc.cam.ac.uk; www: http://www.ccdc.cam.ac.uk/deposit).



## Acknowledgements

This work was conducted in the framework of a project sponsored by the Natural Science Foundation of China (No. 21071100), SRF for ROCS, SEM, and Liaoning BaiQianWan Talents Program and the LNET (LJQ2011038).

## References

[1] P.J. Dandliker, R.E. Holmlin, J.K. Barton. *Science*, **275**, 1465 (1997).
[2] N. Farrell. *Coord. Chem. Rev.*, **232**, 1 (2002).
[3] S. Dhar, D. Senapati, P.K. Das, P. Chattopadhyay, M. Nethaji, A.R. Chakravarty. *J. Am. Chem. Soc.*, **125**, 12118 (2003).
[4] Q. Jiang, N. Xiao, P. Shi, Y. Zhu, Z. Guo. *Coord. Chem. Rev.*, **251**, 1951 (2007).
[5] M. Chikira. *J. Inorg. Biochem.*, **102**, 1016 (2008).
[6] A. Panja, T. Matsuo, S. Nagao, S. Hirota. *Inorg. Chem.*, **50**, 11437 (2011).
[7] J. Qian, W. Gu, H. Liu, F.-X. Gao, L. Feng, S.-P. Yan, D.-Z. Liao, P. Cheng. *Dalton Trans.*, 1060 (2007).
[8] S. Roy, A.-K. Patra, S. Dhar, A.-R. Chakravarty. *Inorg. Chem.*, **47**, 5256 (2008).
[9] S. Ramakrishnan, M. Palaniandavar. *Dalton Trans.*, 3866 (2008).
[10] Y. He, X.-H. Wang, H. Zhou, Z.-Q. Pan, J.-B. Li, Q.-M. Huang. *Inorg. Chem. Commun.*, **13**, 314 (2010).
[11] Y. An, Y.-Y. Lin, H. Wang, H.-Z. Sun, M.-L. Tong, L.-N. Ji, Z.-W. Mao. *Dalton Trans.*, **37**, 1250 (2007).
[12] S. Anbu, M. Kandaswamy, S. Kamalraj, J. Muthumarry, B. Varghese. *Dalton Trans.*, **40**, 7310 (2010).
[13] V. Rajendiran, R. Karthik, M. Palaniandavar, H.-S. Evans, V.-S. Periasamy, M.-A. Akbarsha, B.-S. Srinag, H. Krishnamurthy. *Inorg. Chem.*, **46**, 8028 (2007).
[14] S. Roy, A.-K. Patra, S. Dhar, A.-R. Chakravarty. *Inorg. Chem.*, **47**, 5625 (2008).
[15] R.-S. Kumar, K. Sasikala, S. Arunachalam. *J. Inorg. Biochem.*, **102**, 234 (2008).
[16] E.-J. Gao, T.-D. Sun, S.-H. Liu, S. Ma, Z. Wen, Y. Wang, M.-C. Zhu, L. Wang, X.-N. Gao, F. Guan, M.-J. Guo, F.-C. Liu. *Eur. J. Med. Chem.*, **45**, 4531 (2010).
[17] E.-J. Gao, X.-N. Gao, F. Guan, M.-C. Zhu, L. Liu, M. Zhang, Y.-X. Zhang, Y. Wang, Z. Wen, Y. Zhang, Y. Zhang, Q. Liang. *Eur. J. Med. Chem.*, **46**, 160 (2011).
[18] G.M. Sheldrick. *SHELXS-97, Program For X-ray Crystal Structure Solution*, Göttingen University, Göttingen (1997).
[19] G.M. Sheldrick. *SHELXS-97, Program For X-ray Crystal Structure Refinement*, Göttingen University, Göttingen (1997).
[20] K.-M. Wang, L. Du, J.-M. Han, Z.-Z. Li, M.-J. Xie, Q.-H. Zhao. *Transition Met. Chem.*, **35**, 829 (2010).
[21] Y.-Q. Lan, S.-L. Li, J.-S. Qin, D.-Y. Du, X.-L. Wang, Z.-M. Su, Q. Fu. *Inorg. Chem.*, **47**, 10600 (2008).
[22] G.-P. Yang, Y.-Y. Wang, P. Liu, A.-Y. Fu, Y.-N. Zhang, J.-C. Jin, Q.-Z. Shi. *Cryst. Growth Des.*, **10**, 1443 (2010).
[23] G.-P. Yang, J.-H. Zhou, Y.-Y. Wang, P. Liu, C.-C. Shi, A.-Y. Fu, Q.-Z. Shi. *CrystEngComm*, **13**, 33 (2011).
[24] V. Balamurugan, M.-S. Hundal, R. Mukherjee. *Chem. Eur. J.*, **10**, 1683 (2004).
[25] M.T. Carter, M. Rodriguez, A.J. Bard. *J. Am. Chem. Soc.*, **111**, 8901 (1989).
[26] D.L. Boger, B.E. Fink, S.R. Brunette, W.C. Tse, M.P. Hedrick. *J. Am. Chem. Soc.*, **123**, 5878 (2001).
[27] M. Jiang, Y.-T. Li, Z.-Y. Wu. *J. Coord. Chem.*, **65**, 1858 (2012).
[28] Y.-F. Chen, M. Liu, J.-W. Mao, H.-T. Song, H. Zhou, Z.-Q. Pan. *J. Coord. Chem.*, **65**, 3413 (2012).
[29] Y.-J. Zheng, X.-W. Li, Y.-T. Li, Z.-Y. Wu, C.-W. Yan. *J. Coord. Chem.*, **65**, 3530 (2012).

[30] H.-L. Wu, J.-K. Yuan, Y. Bai, G.-L. Pan, H. Wang, J.-H. Shao, J.-L. Gao, Y.-Y. Wang. *J. Coord. Chem.*, **65**, 4327 (2012).
[31] J.K. Barton, A.L. Raphael. *J. Am. Chem. Soc.*, **106**, 2466 (1984).
[32] H.-L. Ren, C. Wang, J.-L. Zhang, X.-J. Zhou, D.-F. Xu, J. Zheng, S.-W. Guo, J.-Y. Zhang. *ACS Nano*, **4**, 7169 (2010).
[33] D.-D. Li, J.-L. Tian, W. Gu, X. Liu, S.-P. Yan. *Eur. J. Inorg. Chem.*, **2009**, 5036 (2009).
[34] O.A. El-Gammal, G.M. Abu El-Reash, S.E. Ghazy, T. Yousef. *J. Coord. Chem.*, **65**, 1655 (2012).
[35] J.-Z. Lu, H.-W. Guo, Y.-L. Zhang, J. Jiang, Y.-J. Liu, L.-Q. Zang, J.-W. Huang. *J. Coord. Chem.*, **65**, 1765 (2012).
[36] K. Pothiraj, T. Baskaran, N. Raman. *J. Coord. Chem.*, **65**, 2110 (2012).